Building Tomorrow's Society
Bâtir la Société de Demain

Fredericton, Canada
June 13 – June 16, 2018/ *Juin 13 – Juin 16, 2018*

BEHAVIOUR OF FIBRE REINFORCED POLYMER REINFORCED CONCRETE BEAMS WITH FIBRE MESH SHEAR REINFORCEMENT

Shahi, Mridul[1], Tomlinson, Douglas[2,3]
[1] University of Alberta, Canada
[2] University of Alberta, Canada
[3] dtomlins@ualberta.ca

Abstract: Fibre-reinforced polymer (FRP) reinforcement has been used as replacement for steel in concrete structures for many years. Although there are many benefits to using FRP reinforcement, it cannot be bent after fabrication. This causes issues since field adjustments cannot be made as easily as they can with steel reinforcement. This study investigates the effectiveness of a flexible fibre mesh as shear reinforcement in FRP-reinforced concrete structures. Nine 1200 mm long, 155 mm deep concrete T-beams were tested under four-point bending. Test parameters included longitudinal reinforcement (glass FRP with reinforcement ratio, ρ = 0.75%, glass FRP with ρ = 1.19%, and steel with ρ = 1.18%) and shear reinforcement type (steel stirrups with shear reinforcement ratio, ρ_v = 1.51%, 25x25 mm basalt mesh with ρ_v = 0.12%, and no shear reinforcement). A small aggregate (6 mm), high flow concrete mix was used to fabricate the beams since the mesh aperture size is small (25x25) mm. The fibre mesh increased shear resistance relative to beams without shear reinforcement but failure was still governed by shear. This effect was higher (44% increase) in beams with small reinforcement ratios than in beams with larger reinforcement ratios (5% increase). CSA codes (A23.3-14 and S806-12) drastically under-predicted the failure load of beams that failed in shear. The results indicate that fibre mesh can be used as shear reinforcement in concrete structures. However, the use of higher stiffness mesh or additional mesh layers is recommended.

1 INTRODUCTION

Fibre reinforced polymers (FRP) have been used in place of traditional steel reinforcement in concrete structures for several decades. FRP is commonly used in applications where there are severe corrosion concerns, such as in parking structures and bridge decks. FRPs are also used in applications where non-magnetic reinforcement is needed (e.g. hospital MRI rooms) as wall as where low thermal conductivities are preferred (e.g. shear connectors in insulated concrete wall panels) (ACI 2015). The use of FRP reinforcement in Canada has been codified for over 15 years in both building (CSA S806-12) and in bridge (CSA S6-14) design.

Glass FRP (GFRP) is the most popular FRP type used in civil engineering applications. Glass is popular since it has a good balance of material properties and cost (ACI 2015). Another type of fibre, basalt, has been gaining more interest in research applications. Basalt fibres are slightly stiffer and stronger than glass fibres and the design of basalt FRP reinforced structures has been found to follow the same process as GFRP reinforced structures (Tomlinson and Fam, 2014).

Though FRP is stronger than steel reinforcement, it has a low stiffness as well as a brittle failure mode. This lower stiffness means that FRP reinforced flexural members are often governed by serviceability (i.e. crack width and deflections) rather than flexural strength considerations. The lower reinforcement stiffness

also means that FRP-reinforced structures are more likely to fail in shear (El-Sayad et al. 2005, Bentz et al. 2010). Although serviceability-related issues with FRP are accounted for in design codes, FRP bars also cannot be bent after they are fabricated. This creates issues if field adjustments are required and is particularly a concern when using pre-bent shear reinforcement.

An alternative to using FRP stirrups is to use a fibre mesh. Fibre mesh is more flexible than FRP bars so it can be adjusted in the field. Fibre mesh has successfully been used as shear connectors in insulated concrete wall panels and as flange reinforcement in precast concrete double-tees (Lunn et al. 2015). However, there is very little available information on the performance of fibre mesh as shear reinforcement in concrete structures. This paper investigates if a commercially available basalt fibre mesh can be used as shear reinforcement in concrete beams.

2 EXPERIMENTAL PROGRAM

2.1 Description Specimens and Testing Matrix

The feasibility of basalt mesh as shear reinforcement was evaluated using nine small-scale reinforced concrete T-beams (Figure 1). The T-beams were 1200 mm long with a total depth of 155 mm. The beam flanges were 250 mm wide and 55 mm thick. T-beams were used rather than a rectangular section as they are more likely to fail in shear (the concrete shear contribution, V_c, is proportional to web thickness).

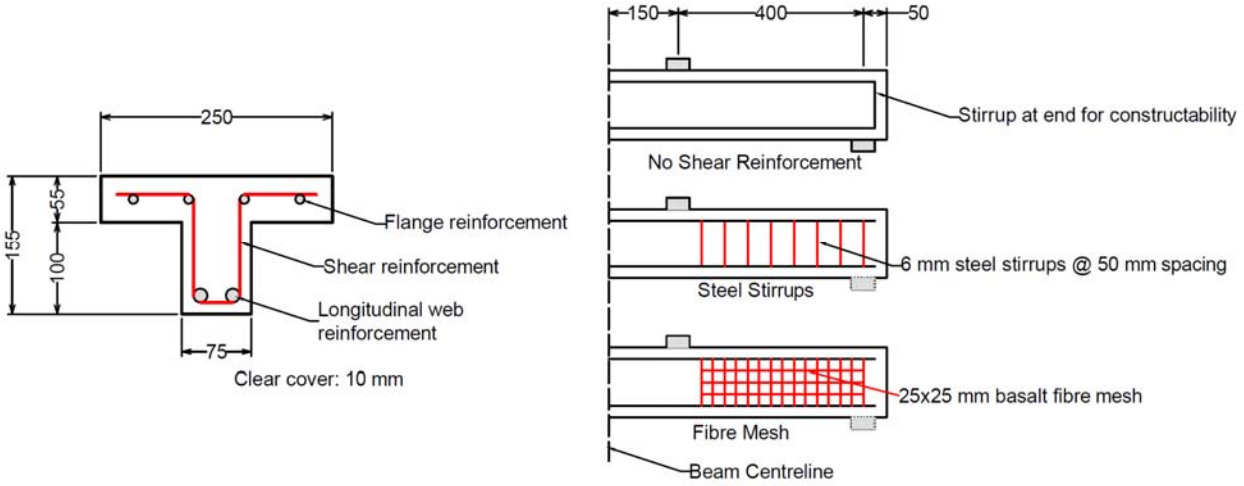

Figure 1: Beam designs showing cross section layout and shear reinforcement types. All dimensions in mm.

The test matrix for the beams is shown in Table 1. Each beam had a different combination of flexural and shear reinforcement. Three types of longitudinal reinforcement were used: 2x15M steel bars, 2x#4 GFRP bars, and 2x#5 GFRP bars. Based on the provided cover (10 mm) and stirrup size (6 mm), the reinforcement depth, d, was 133 mm for the beams with #4 bars and 131 mm for the beams with #5 and 15M bars. The reinforcement ratios, ρ, for the beams ranged from 0.75% to 1.19% and were compared to the balanced reinforcement ratio, ρ_b, found using equation [1].

$$[1]\ \rho_b = \frac{\alpha_1 f_c' \beta_1}{f_y}\left(\frac{\varepsilon_{cu}}{\varepsilon_{cu}+\varepsilon_y}\right)$$

Where α_1 and β_1 are concrete stress block modifiers calculated using CSA A23.3-14, f_y is the steel yield strength, ε_{cu} is the concrete crushing strain (taken as 0.0035 as per CSA codes), and ε_y is the steel yield strain. For GFRP-reinforced beams, f_y and ε_y were replaced by the GFRP tensile strength and rupture strain.

The steel-reinforced beams have a ρ equal to $0.23\rho_b$, making the beam under-reinforced. This ρ is representative of reinforcement ratios typically used in steel-reinforced concrete beams. The GFRP-reinforced beams had ρ equal to $1.74\rho_b$ (using #4 bars) or $2.73\rho_b$ (using #5 bars). Both GFRP-reinforced beam designs are over-reinforced which is preferred for FRP-reinforced sections. The GFRP reinforcement ratios were chosen to either match ρ of the steel-reinforced beam (#5 bars) or to match the theoretical flexural capacity of the steel-reinforced beam (#4 bars).

Three types of shear reinforcement were used. The first type, 6 mm diameter steel stirrups spaced at 50 mm, gave a shear reinforcement ratio, ρ_v, of 1.51%. These beams were designed with excessive shear reinforcement to ensure that they did not fail in shear-tension and serve as the upper bound capacity for the beam design. The second type, unreinforced, has no shear reinforcement (i.e. $V_r = V_c$). These beams are intended to fail in shear (i.e. gives a lower bound capacity for the beams). The last type, basalt fibre mesh with a shear reinforcement ratio of 0.12%, was chosen as a balance between mesh area and for constructability considerations. The effectiveness of the mesh can be evaluated by comparing the response of the beams with mesh reinforcement to those of the other beams.

Table 1: Test matrix

Test ID*	Longitudinal Reinforcement				Shear Reinforcement		
	Material	Bar Size (mm)	Reinforcement Ratio, ρ (%)	ρ/ρb	Material	Spacing (mm)	Ratio, ρ_v (%)
SN-1.2	Steel	16	1.19	0.23	None	N/A	0
SS-1.2	Steel	16	1.19	0.23	Steel	50	1.51
SB-1.2	Steel	16	1.19	0.23	BFRP	25	0.12
GN-0.8	GFRP	13	0.75	1.74	None	N/A	0
GS-0.8	GFRP	13	0.75	1.74	Steel	50	1.51
GB-0.8	GFRP	13	0.75	1.74	BFRP	25	0.12
GN-1.2	GFRP	15	1.17	2.73	None	N/A	0
GS-1.2	GFRP	15	1.17	2.73	Steel	50	1.51
GB-1.2	GFRP	15	1.17	2.73	BFRP	25	0.12

*Specimens were identified based on their longitudinal reinforcement material (S – steel, G – GFRP), shear reinforcement material (N – none, S – steel stirrups, B – basalt fibre mesh), and longitudinal reinforcement ratio, rounded to the nearest 10th of a percent (0.8 or 1.2).

2.2 Material Properties

The reinforcement used in the beams is shown in Figure 2.

Figure 2: Reinforcement used in beams (a) Steel rebar (b) GFRP bars (c) Basalt mesh

2.2.1 Steel reinforcement and stirrups

Two sizes of Grade 400 (f_y = 400 MPa, E_s = 200 GPa) steel rebar were used. 10M bars (A_s = 100 mm^2) were used as compression reinforcement in the beam flanges while 15M bars (A_s = 200 mm^2) were used as longitudinal reinforcement in the webs. The steel stirrups were 6 mm diameter (A_s = 31 mm^2) smooth bars.

2.2.2 Glass Fibre Reinforced Polymer Bars

Three GFRP bar sizes were used. #3 bars (nominal diameter of 10 mm and area of 71 mm^2) were used as reinforcement in the flange. #4 bars (nominal diameters and area of 13 mm and 129 mm^2) were used as tension reinforcement in the beams with ρ = 0.75%; #5 bars (nominal diameters and areas of 15 mm and 199 mm^2) were used as tension reinforcement in the beams with ρ = 1.18%. The manufacturer provided properties were f_u = 983.8 MPa and E_f = 49.1 GPa for the #3 bars, f_u = 1175 MPa and E_f = 61.1 GPa for the #4 bars, and f_u = 1150 MPa and E_f = 62.6 GPa for the #5 bars.

2.2.3 Basalt Fibre Mesh

The basalt fibre mesh was composed of 2 mm thick strands with a centre-to-centre aperture size of 25×25 mm. The manufacturer provided properties of the mesh were f_u = 1800 MPa, E_f = 70 GPa, and unit strength of 80 kN/m.

2.2.4 Concrete

The concrete mix, shown in Table 2, has a design strength, f_c', of 50 MPa. The concrete was designed to be self-consolidating with a water/cementitious materials ratio of 0.36 and a maximum nominal aggregate size of 6 mm. A water reducing admixture was used to increase the slump of the concrete and make it self-consolidating. The small aggregates and high flow of the mix were desired as this allows the concrete to flow between apertures in the basalt fibre mesh. The concrete mix had a flow of 575 mm and was found to be non-segregating. The tested concrete cylinder strength for all of the beams (3 cylinders per beam) was 46.6 MPa with a standard deviation of 4.9 MPa.

Table 2: Concrete mix design

Material	Quantity (kg)
Water	9.2
Cement	19.4
Coarse aggregate	25.4
Fine aggregate	22.4
Fly ash	6.3
Water reducing admixture	0.135

2.3 Fabrication of Test Specimens

The fabrication process for the beams with basalt fibre mesh is illustrated in Figure 3.

1. The reinforcement was cut to length and cages were tied (Figure 3(a)). FRP bars were cut using a diamond-bladed saw while the basalt fibre mesh was cut using scissors. FRP sections were tied with plastic zip-ties.
2. After the cages were constructed they were added to the forms and concrete was batched (Figure 3(b)) using a small-capacity drum mixer. Each beam was cast using a different batch of concrete.
3. Concrete was added to the forms and flowed around the reinforcement and fibre mesh. During casting, it was observed that concrete was able to flow through the mesh apertures (Figure 3(c)). To prevent concrete from shifting the mesh too much during casting, it is recommended that concrete be poured on both sides of the mesh during casting to limit pressure differentials.

4. After casting, the beams were cured under a plastic sheet and stripped from their forms after one week (Figure 3(d)).

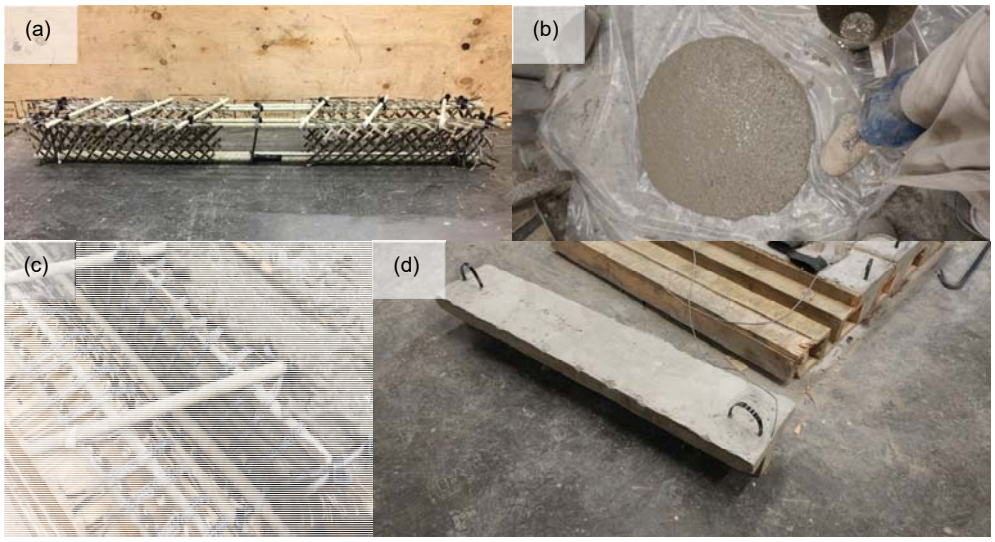

Figure 3: Fibre mesh beam fabrication process (a) tied reinforcement cage, (b) fresh self-consolidating concrete (c) concrete placed around fibre mesh (d) constructed beam ready for testing.

2.4 Test Setup and Instrumentation

The test setup is shown in Figure 4. Each beam was tested in four-point bending with a span of 1100 mm. The shear span of the beams was 400 mm (a/d ratio of 3.0, typical in beam testing (Machial et al. 2012)). The beams were loaded under displacement control at a rate of 1 mm per minute. Loads were measured using a load cell mounted on the actuator while midspan displacements were measured using a cable transducer. Digital cameras were set up on a time-lapse to take photos of each shear span and track crack propagation.

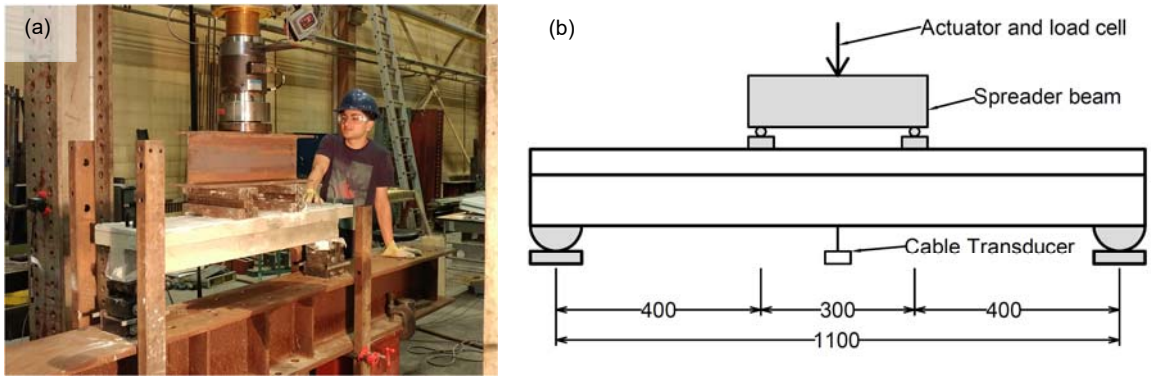

Figure 4: Test setup and instrumentation (a) photo of beam immediately before testing (b) diagram showing load points and instrumentation. All dimensions in mm.

3 RESULTS

3.1 Load-Deflection Relationships up to failure

The load-deflection relationships for each test are shown in Figure 5 with the results summarized in Table 3. Regardless of reinforcement type, all beams had similar pre-cracked stiffness and cracking loads (around 10 kN). After cracking, the stiffness of each beam decreased substantially as expected. The post-cracking stiffness was roughly proportional to the axial stiffness of the longitudinal reinforcement. In all beams, the

first major shear cracks formed at loads between 30 and 40 kN. After this point, beams with stirrups (SS-1.2, GS-0.8, and GS-1.2) had negligible decrease in their stiffness. Beams without stirrups then had noticeably higher deflections than those with stirrups after this point with the decrease being highest for GN-0.8 and lowest for SN-1.2, showing that the loss in stiffness after initial formation of shear cracking is proportional to the axial stiffness of the longitudinal reinforcement. The fibre mesh, however, behaved differently. The mesh was most effective when the axial stiffness of the longitudinal reinforcement was low (GB-0.8) but became less effective as the axial stiffness of the longitudinal reinforcement increased.

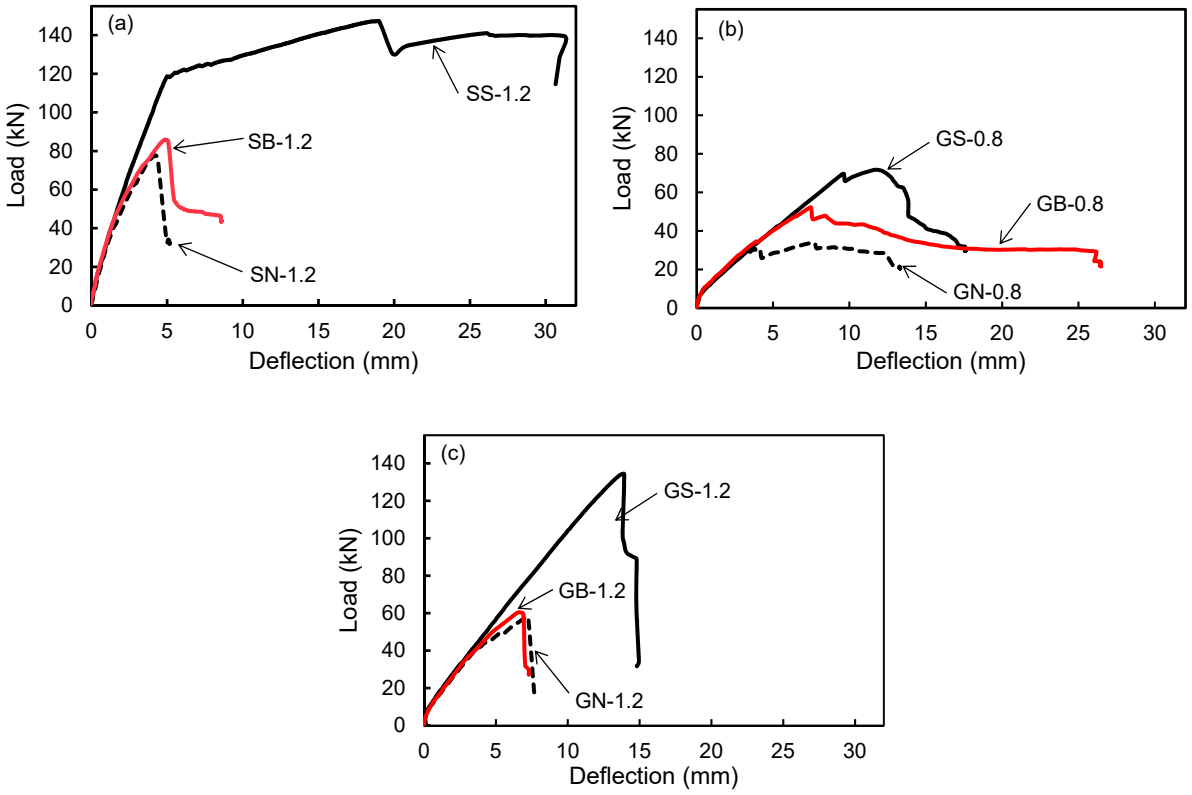

Figure 5: Load-deflection relationships for the tested beams (a) steel longitudinal reinforcement, (b) GFRP longitudinal reinforcement (ρ = 0.75%), (c) GFRP longitudinal reinforcement (ρ = 1.19%)

Table 3: Experimental Results

Test ID	Concrete Strength, MPa	Load at L/360, mm	Peak Load, kN	Deflection at Peak Load, mm	Failure Mode
SN-1.2	45.6	64.9	77.8	4.22	Shear-Tension
SS-1.2	50.9	80.1	147.3	19.0	Concrete Crushing after steel yields
SB-1.2	50.5	68.4	85.9	4.86	Mesh Rupture
GN-0.8	44.8	28.0	33.8	3.81	Shear-Tension
GS-0.8	40.8	27.6	71.7	11.8	FRP Bond Slip
GB-0.8	51.8	29.4	52.3	7.47	Mesh Rupture
GN-1.2	52.5	35.6	58.2	7.27	Shear-Tension
GS-1.2	42.0	37.8	134.5	13.9	Web Crushing
GB-1.2	45.0	36.8	60.4	6.75	Mesh Rupture

3.2 Failure Modes

Five failure modes were observed and are shown in Figure 6. Failure of the beams without shear reinforcement was by shear-tension, as expected. This failure mode was sudden and generally gave little warning that it was about to occur. An exception was in GN-0.8, which showed a pseudo-plateau after initial failure, which has been observed in similar beams with relatively low reinforcement ratios (Tomlinson and Fam, 2014). The beams with basalt mesh failed by mesh rupture. This failure had a similar appearance to shear tension failure but was preceded by sounds of mesh failure. Additionally, the post-failure load (where the load stabilizes after the first major failure) of the mesh-reinforced beams was higher than those of the beams without shear reinforcement, indicating that not all mesh strands intercepting the crack failed. The beams with steel stirrups failed by either concrete crushing after steel yield (SS-1.2), diagonal failure of the concrete struts (GB-1.2), or pullout failure (GB-0.8). The premature failures of the FRP-reinforced beams are attributed to their relatively low concrete strengths (40.8 MPa for GS-0.8 and 42.0 MPa for GB-1.2).

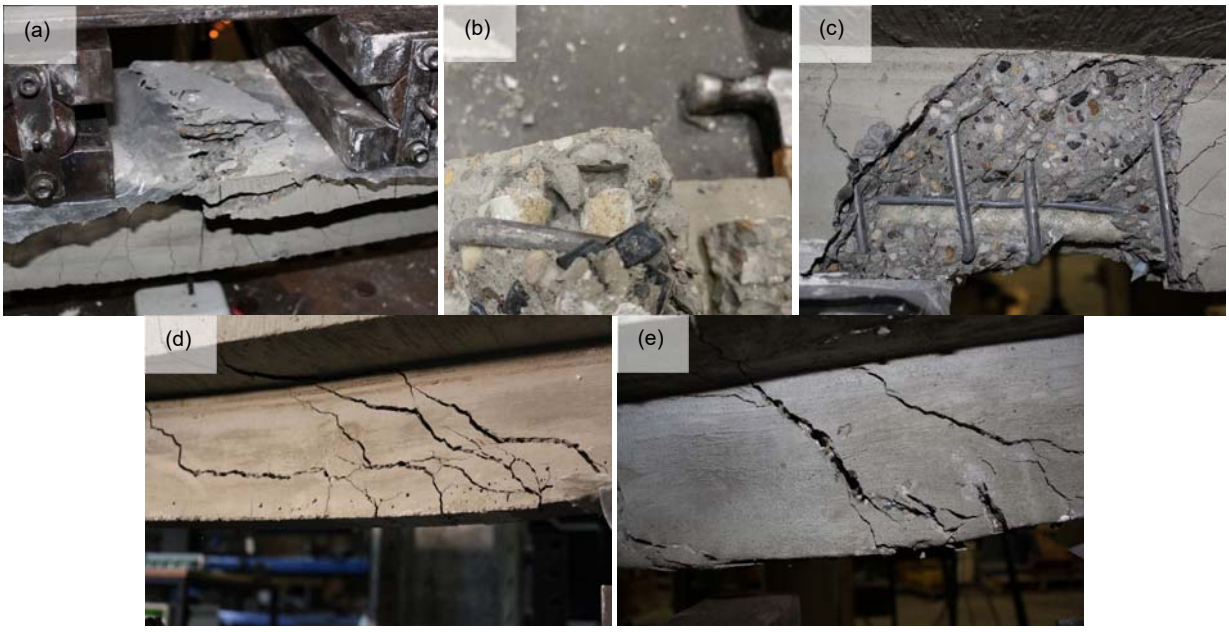

Figure 6: Failure modes of specimens (a) concrete crushing in SS-1.2, (b) FRP pullout at support of GS-0.8 (c) web crushing in GS-1.2, (d) shear-tension failure in GN-0.8, (e) fibre mesh rupture in GB-0.8

4 DISCUSSION

The shear performance of concrete members with various concrete strengths is often compared by normalizing the shear force (Machial et al. 2012). Shear forces are normalized using equation [2].

[2] $V_{norm} = V_{ult}/\sqrt{f_c'}b_w d$

Where V_{norm} is the normalized shear resistance (MPa), V_{ult} is the maximum shear force achieved in the test (N), and b_w is the width of the concrete web (mm). The normalized shear is plotted (Figure 7) against the normalized axial stiffness of the tension reinforcement, $n\rho$, of the beams to account for the different modulus of elasticity of the GFRP and the steel. The modular ratio, n, was determined by dividing the reinforcement material properties reported earlier by the concrete elastic modulus, E_c, calculated using A23.3-14.

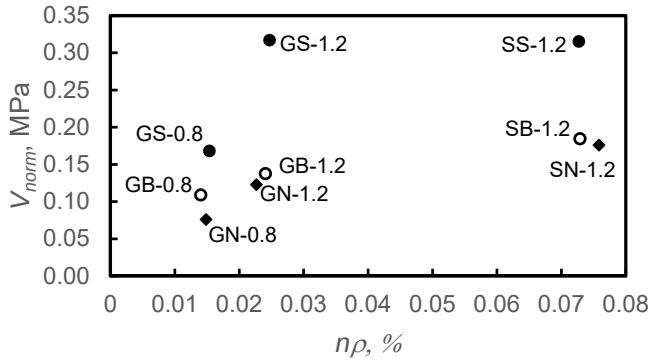

Figure 7: Normalized shear versus normalized axial stiffness for the tested beams

Unlike steel-reinforced concrete, FRP members do not show ductility. For FRP members, a similar concept, deformability, is used to relate how the ultimate performance of the beam relates to its service performance. For each beam, deformability was evaluated using equation [3].

[3] $\Psi = M_u\delta_u/M_s\delta_s$

Where Ψ is the deformability index, M_u is the ultimate moment, δ_u is the deflection at ultimate, M_s is the service load moment, and δ_s is the service load deflection. For this beam, the service load was taken as the load at a deflection of L/360, which is commonly used as an allowable service deflection limit in concrete structures. The results of this, along with how the beams relate to predictions from CSA codes, is presented in Table 4.

Table 4: Beam performance

Test ID	Test ultimate load, kN	Normalized shear resistance, V_n	Deformability Index	Ultimate load predicted by CSA codes, kN	Test/predicted ratio
SN-1.2	77.8	0.176	1.66	24	3.24
SS-1.2	147.3	0.315	11.4	117	1.26
SB-1.2	85.9	0.184	2.00	30	2.86
GN-0.8	33.8	0.075	1.51	27	1.25
GS-0.8	71.7	0.168	10.0	101	0.71
GB-0.8	52.3	0.109	4.35	31	1.68
GN-1.2	58.2	0.122	3.89	27	2.16
GS-1.2	134.5	0.317	16.2	138	0.97
GB-1.2	60.4	0.137	3.62	34	1.78

Shear-tension failure was prevented in the beams reinforced with steel stirrups (ρ_v=1.51%). This indicates that the stirrups were fully effective at preventing failure. The beams without shear reinforcement all failed in shear at considerably lower loads (decrease in V_{norm} of between 39 and 56%) than the beams with stirrups. The basalt mesh gave higher capacities than the beams without stirrups but the gain was very small for SB-1.2 (5%) as well as in GB-1.2 (12%). The higher contribution of the mesh in GB-0.8 (44%) shows that fibre mesh is more effective for beams with lower axial stiffness of reinforcement.

The basalt mesh tended to improve the deformability and service load of the beams relative to the beams without stirrups. Prior to mesh rupture, it limited the width of the critical shear crack and this allowed higher loads (and deflections) than those seen in beams without stirrups. However, the mesh reinforcement was considerably less effective than the steel stirrups at improving deformability. A major reason for this is that the mesh has a small cross-sectional area per layer. Either more layers of mesh or a higher capacity (strength and stiffness) mesh is required to shift the failure mode from mesh rupture to flexure. For T-

beams, it is recommended that deformability values exceed 6 (CSA S6). This is achieved with the beams with steel stirrups (all have values over 10) but was not achieved by any of the other beams.

The mesh's effectiveness is limited by its relatively small cross-section and stiffness relative to the steel stirrups. Future testing should include higher stiffness material (e.g. use of carbon rather than basalt), or increased area of mesh (e.g. adding a second mesh layer). However, for constructability purposes, reducing the aperture of the mesh below 25 mm is not recommended since smaller apertures may lead to concrete placement issues.

Shear resistance increases with longitudinal reinforcement stiffness ($n\rho$). This is expected since higher stiffness reinforcement limits the size of shear cracks and encourages higher amounts of aggregate interlock, leading to higher shear capacities (Bentz et al. 2010).

Each beam was also compared to predictions from A23.3-14 (steel reinforced concrete beams) and S806-12 (GFRP-reinforced concrete beams). Predictions were made using material reduction factors set to unity. The beams that failed in shear had considerably higher capacities than those predicted by CSA codes (with the test/CSA ratio ranging from 1.25 to 3.24). Some of this increase is linked to scaling effects, since smaller beams tend to have higher shear capacities than larger ones (Bentz et al. 2010). However, it is also seen that the CSA predictions for the beams that failed in shear become worse as reinforcement stiffness increases.

5 CONCLUSIONS AND RECOMMENDATIONS

Nine small-scale concrete beams reinforced with various longitudinal and shear reinforcement types were tested in bending. The following was concluded from this study:

1. Beams with fibre mesh shear reinforcement can be constructed using a similar technique to typical beams. It is recommended that concrete used in these beams have a high flow and small aggregates (~1/4 the size of the centre-to-centre mesh aperture size) to allow it to pass through mesh apertures. It is also recommended to pour concrete on both sides of a mesh to prevent it from shifting during casting.
2. Basalt fibre mesh increases shear resistance of beams relative to those without shear reinforcement but this increase is relatively small, particularly for beams with relatively high reinforcement stiffness. Either more layers of reinforcement or a higher stiffness material are required to get significant shear contributions when using fibre-mesh as shear reinforcement.
3. The mesh limited the size of the shear cracks prior to rupture. This indicates that fibre mesh is effective at controlling cracking in concrete beam webs. Additionally, the bi-directional nature of the mesh ensures that angled cracks are intercepted.
4. CSA codes underestimated the shear resistance of the beams that failed in shear.

The authors recommend the testing and modelling of full scale beams reinforced with fibre mesh to evaluate the performance of the mesh in larger structures. They also recommend testing different fibre mesh types (e.g. carbon) and arrangements (e.g. multiple layers) in future testing. Future studies should also investigate how effective fibre mesh is at controlling crack widths.

Acknowledgements

The authors wish to thank the Structural Engineering Technical Staff in the Morrison Structures Lab at the University of Alberta (Greg Miller and Cameron West) as well as Sylvester Agbo (PhD Student at the University of Alberta).

References

American Concrete Institute (ACI) Committee 440. 2015. *Guide for the Design and Construction of Structural Concrete Reinforced with Fiber-reinforced Polymer (FRP) bars,* ACI, Farmington Hills, MI, USA.

Bentz, E.C., Massam, L. and Collins, M.P. 2010. Shear Strength of Large Concrete Members with FRP Reinforcement. *Journal of Composites for Construction*, ASCE, **14**(6):637–646.

Canadian Standards Association (CSA). 2012. *Design and Construction of Building Structures with Fibre-Reinforced Polymers – CAN/CSA S806-12*, CSA, Mississauga, ON, Canada.

Canadian Standards Association (CSA). 2014. *Design of Concrete Structures – CAN/CSA A23.3-14*, CSA, Mississauga, ON, Canada.

El-Sayed, A., El-Salakawy, E. and Benmokrane, B. 2005. Shear Strength of One-Way Concrete Slabs Reinforced with Fiber-Reinforced Polymer Composite Bars. *Journal of Composites for Construction* **9** (2):147–157.

Lunn, D, Lucier, G., Rizkalla, S., Cleland, N. and Gleich, H. 2015. New Generation of Precast Concrete Double Tees Reinforced with Carbon-Fiber-Reinforced Polymer Grid. *PCI Journal*, PCI, **45**(4):37–48.

Machial, R., Alam, M.S. and Rteil, A. 2012. Revisiting the Shear Design Equations for Concrete Beams Reinforced with FRP rebar and Stirrup. *Materials and Structures*, **45**(11):1593–1612.

Tomlinson, D. and Fam, A. 2014. Performance of Concrete Beams Reinforced with Basalt FRP for Flexure and Shear. *Journal of Composites for Construction*, ASCE, **19**(2):04014036.